Published for SISSA by Springer

Received: *May 8, 2012*
Revised: *July 23, 2012*
Accepted: *July 24, 2012*
Published: *August 1, 2012*

Reach the bottom line of the sbottom search

Ezequiel Álvarez[a,b] **and Yang Bai**[b]

[a] *CONICET, INFAP and Departamento de Física, FCFMN, Universidad Nacional de San Luis, Av. Ejército de los Andes 950, 5700, San Luis, Argentina*
[b] *SLAC National Accelerator Laboratory, 2575 Sand Hill Road, Menlo Park, CA 94025, U.S.A.*

E-mail: sequi@df.uba.ar, yangbai@slac.stanford.edu

Abstract: We propose a new search strategy for directly-produced sbottoms at the LHC with a small mass splitting between the sbottom and its decayed stable neutralino. Our search strategy is based on boosting sbottoms through an energetic initial state radiation jet. In the final state, we require a large missing transverse energy and one or two b-jets besides the initial state radiation jet. We also define a few kinematic variables to further increase the discovery reach. For the case that the sbottom mainly decays into the bottom quark and the stable neutralino, we have found that even for a mass splitting as small as 10 GeV sbottoms with masses up to around 400 GeV can be excluded at the 95% confidence level with 20 inverse femtobarn data at the 8 TeV LHC.

Keywords: Hadronic Colliders, Supersymmetry Phenomenology

ArXiv ePrint: 1204.5182

doi:10.1007/JHEP08(2012)003

Contents

1 Introduction

With the recent discovery of a narrow resonance of mass 125 GeV [1–3], which seems to be the long-sought Higgs boson, the Large Hadron Collider (LHC) has entered an exciting era for understanding the physics of electroweak symmetry breaking. If this new particle is the Higgs boson, then the next big goal is to look for physics beyond the standard model that makes a light Higgs boson natural and (or) explains the large hierarchy between the fundamental Planck scale and the electroweak scale. One of the beyond-the-standard models that naturally explains the lightness of the Higgs boson is supersymmetry (SUSY). To cancel the large radiative corrections to the Higgs mass in the SM from the top quark loop without fine tuning, the top superpartners (stops) need to be light enough [4, 5]. There are increasing amount of interests in the literature on generating SUSY spectra with a light stop from model-building or improving stop searches at the LHC from collider studies (see ref. [6] for a recent review). Noticing that the left-handed stop and the left-handed sbottom belong to a weak doublet, their masses should be naturally comparable. Light stops below 1 TeV implicitly imply at least one sbottom below around 1 TeV. Therefore, searching for sbottoms is equally important for us to understand the electroweak symmetry breaking in SUSY [7].

Sbottoms could be directly produced in pairs at hadron colliders from their QCD interaction. With an unbroken R-parity and a stable neutralino $\tilde{\chi}$ as the lightest supersymmetric particle (LSP), the dominant decay channel for the lighter sbottom is $\tilde{b}_1 \to b\tilde{\chi}$. For the parameter space with a large mass difference between sbottom and neutralino, the standard signature for the direct sbottom search is two jets containing at least one b-jet plus a large missing energy $E_T^{\rm miss}$. By requiring at least one b-jet in the final state, the existing search from CDF with 2.65 fb^{-1} of integrated luminosity has excluded sbottom masses up to 230 GeV for neutralino masses below 70 GeV at 95% confidence level (C.L.) [8]. With a larger luminosity of 5.2 fb^{-1} and requiring two b-jets, the D0 collaboration has set a 95% C.L. lower limit on the sbottom mass to be 247 GeV for the neutralino mass below

JHEP08(2012)003

40 GeV [9]. At the 7 TeV LHC, the ATLAS collaboration has performed a search of the sbottom particle in 2.05 fb^{-1} and extended the limits on the sbottom mass to be 390 GeV for neutralino masses below 60 GeV [10].

The existing searches on sbottoms (i.e., ref. [10]) do not cover a wide range of sbottom and neutralino mass parameter space when their masses are close to each other. In this paper, we explore alternative search strategies to fill this gap and hope to cover the region for the mass difference of sbottom and neutralino reaching to almost the bottom quark mass. For this compressed or squeezed spectrum, the traditional search strategy by requiring a large transverse missing energy with two b-jets (see ref. [11] and [12] for recent collider studies) is not optimized because $E_T^{\rm miss}$ and the p_T of the leading b-jet decrease as the mass splitting decreases. However, if one requires one additional hard jet from the initial state radiation (ISR), the situation will be different because the two neutralino's in the decaying products are not only boosted but also move in a direction close to each other. As a result, the total transverse missing energy can be sufficiently large to reduce the SM backgrounds. The basis of this idea was already explored in ref. [13] in another context.

One might think that the mono-jet search results can be used to cover the squeezed spectrum [14, 15]. This is indeed the case for a light sbottom with a large production cross section. However, the mono-jet search is still not the optimized one to cover a large fraction of the sbottom-neutralino mass parameter space because of the large Z plus jets background. To extend the search limit of sbottom, we propose a new search strategy in this paper by requiring one energetic non b-tagged jet from the ISR, a large transverse missing energy and one (or two) b-tagged jet with a modest transverse energy. Other than the proposal of this general search strategy, we also explore additional good kinematic variables to further reduce the SM backgrounds.

Our paper is organized as following. We first study the boost of sbottoms from an ISR jet and discuss the general search strategy in section 2. Then, we explore and present three additional variables to further cut the SM backgrounds in section 3. In section 4, we show the discovery reach and compare our search strategy with the existing strategy for the squeezed spectrum. We discuss other issues and conclude our paper in section 5.

2 Boosting the sbottom from an ISR jet

One of the existing searches of sbottoms at ATLAS is based on the direct production of a pair of sbottoms using the decay channel $\tilde{b}_1 \to b + \tilde{\chi}$ [10]. In their search, they require two b-tagged jets with $p_T(b_1) > 130$ GeV (b_1 representing the leading b-jet) and $p_T(b_2) > 50$ GeV on top of the missing energy cut $E_T^{\rm miss} > 130$ GeV. One variable called the boost-corrected contransverse mass, $m_{\rm CT} \equiv ([E_T(v_1) + E_T(v_2)]^2 - [\mathbf{p_T}(v_1) - \mathbf{p_T}(v_2)]^2)^{1/2}$, has been introduced to further reduce the backgrounds. Based on 2.05 fb^{-1} of data at $\sqrt{s} = 7$ TeV, sbottom masses up to 390 GeV are excluded at 95% C.L. for $m_{\tilde{\chi}} < 60$ GeV and Br$(\tilde{b}_1 \to b\tilde{\chi}) = 100\%$. From figure 2 of ref. [10], one can see that the current search strategy at ATLAS has not yet covered a wide region of parameter space for $\Delta m \equiv m_{\tilde{b}_1} - m_{\tilde{\chi}}$ between the bottom quark mass m_b and around 150 GeV.

JHEP08(2012)003

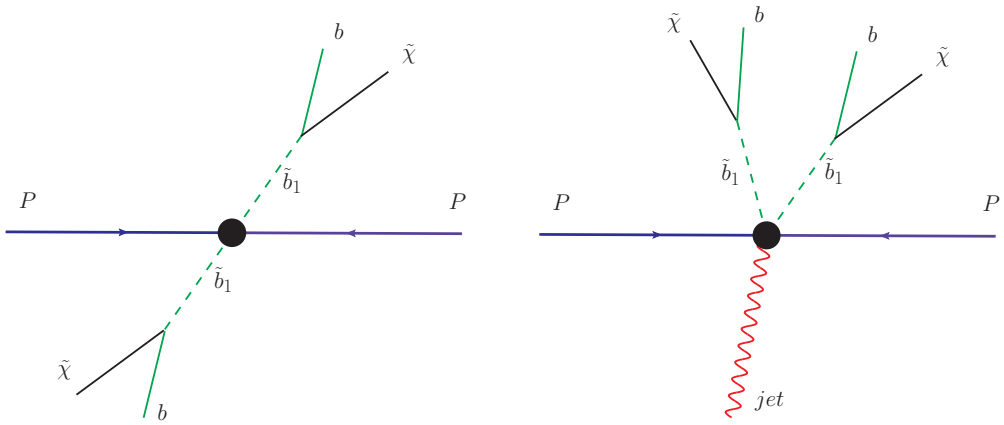

Figure 1. Left panel: a schematic plot for the pair-production of sbottoms at the LHC. Right panel: the pair-production of sbottoms together with an energetic ISR jet.

The reason for the limitation of the ATLAS searches on the squeezed spectrum is two-fold. First, when Δm is small compared to the neutralino mass, the momentum of $\tilde{\chi}$ in the rest frame of $\tilde{b}_1$ is Δm after neglecting the bottom quark mass m_b. If there is no additional jet to boost the two-$\tilde{b}_1$ system in the transverse direction, as illustrated in the left panel of figure 1, the missing transverse energy $E_T^{\rm miss}$ should be bounded by $2\Delta m$, with the upper limit reached when both neutralinos are moving in the same direction perpendicular to the beam direction. To passing the cut on $E_T^{\rm miss}$, a large mass splitting is required. Similar arguments hold for the momenta of two b's. In the rest frame of $\tilde{b}_1$, the momentum of b is around Δm. To passing the stringent cut with $p_T(b_1) > 130\,{\rm GeV}$, one basically requires to have $\Delta m \gtrsim 130\,{\rm GeV}$ if the sbottoms are not moving too fast in the center of mass frame and there is no additional jets to boost sbottoms in the transverse direction.

The story changes if there is an additional ISR jet with a large transverse momentum. The two-$\tilde{b}_1$ system turns to move in the transverse direction opposite to the ISR jet, as depicted in the right panel of figure 1. For an ISR jet with a transverse momentum $p_T(j_1) < m_{\tilde{b}_1}$ and for a small mass splitting Δm, the sum of neutralino's transverse momenta is around $p_T(j_1)$ and hence can pass a stringent cut on the missing transverse momentum. For the two b's in the final state, one can have the leading b-jet with a transverse momentum as large as $(1 + p_T(j_1)/m_{\tilde{b}_1})\Delta m$ if one sbottom does not move in the transverse direction, and the summation of the $p_T(b_1)$ and $p_T(b_2)$ to be $(2+p_T(j_1)/m_{\tilde{b}_1})\Delta m$. At hadron colliders, the pair-produced sbottoms also have non-negligible velocities in the transverse direction. As a result, the b jets produced from sbottom decays can easily pass the minimum kinematic requirement like $p_T(b_1) > 25\,{\rm GeV}$. However, it is very rare to pass the very stringent cut like $p_T(b_1) > 130\,{\rm GeV}$, imposed in the current ATLAS search [10], for the squeezed spectrum. So, we propose a new search strategy to cover the squeezed mass spectra with a small value of Δm by requiring the following three basic objects in the final state:

- *One energetic non b-tagged jet from the initial state radiation.*
- *A large transverse missing energy.*
- *A b-tagged jet with a modest transverse energy.*

JHEP08(2012)003

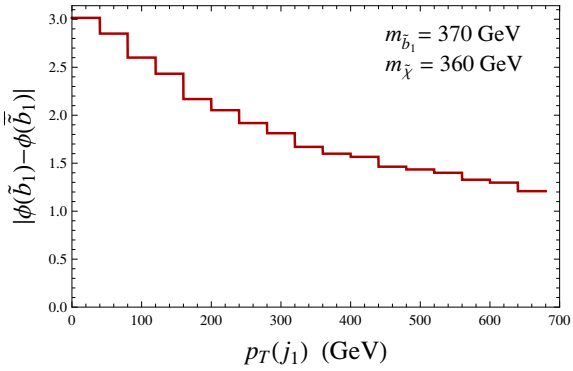

Figure 2. The parton-level distribution of the averaged azimuthal angle difference of two sbottoms in terms of the ISR jet p_T.

On top of those three basic requirements, we will also explore other kinematic variables to further improve the search limit of squeezed sbottom spectra.

Since the LHC is currently running with 8 TeV center-of-mass energy, all our simulation and estimation will be based on the 8 TeV LHC. We simulate signal and background events using `MadGraph5` [16], and shower them in `PYTHIA` [17]. We use `PGS` [18] to perform the fast detector simulation, after modifying the code to implement the anti-k_t jet-finding algorithm with the distance parameter $R = 0.4$ [19]. To avoid the double counting issue, the background events are simulated using a parton shower plus matrix element matched method with the MLM scheme [20] implemented in `MadGraph5`. The signal production cross section is normalized to be the value calculated at NLO+NLL [21]. We choose the branching ratio of $\tilde{b}_1 \to b\tilde{\chi}$ to be 100%. The main backgrounds for our analysis contain $t\bar{t}$ in semileptonic and dileptonic channels, single top production plus jets, $Wbbj$ and $Zbbj$ (we call $V + bb$ backgrounds later). The background production cross section for $t\bar{t}$ is normalized to have a k-factor 1.7, calculated approximately at NNLO [22]. In our studies, the leptonic decays of the top quarks contain $\tau^{\pm}$ leptons. For other backgrounds, we use the k-factor 1.1 for the single top background [23], 1.7 for the $Zbbj$ background [24] and 2.0 for the $Wbbj$ background [25].

To illustrate the effects of the ISR jet on the kinematics of sbottoms, we show the averaged azimuthal angle difference, $|\phi(\tilde{b}_1) - \phi(\bar{\tilde{b}}_1)|$, as a function of the ISR jet p_T's in figure 2. From this figure, one can see that for a small value of $p_T(j_1)$ the two sbottoms produced prefer to be back-to-back in the transverse direction and have the averaged azimuthal angle difference to be close to π, while for a large value of $p_T(j_1)$ they turn to move in the same direction with a smaller value of $|\phi(\tilde{b}_1) - \phi(\bar{\tilde{b}}_1)|$. The distribution of $|\phi(\tilde{b}_1) - \phi(\bar{\tilde{b}}_1)|$ confirms our schematic plots of the signal production mechanism in Fig 1. For the squeezed spectra, the missing transverse energy is approximately opposite to the ISR jet p_T with the same magnitude. Therefore, the averaged $|\phi(\tilde{b}_1) - \phi(\bar{\tilde{b}}_1)|$ distribution as a function of the $E_T^{\rm miss}$ has a similar distribution as in figure 2. With a large missing energy cut, the two sbottoms are not back-to-back and hence the $m_{\rm CT}$ cut introduced for the case without ISR is not useful to cover the squeezed spectrum case.

JHEP08(2012)003

3 Additional variables to reduce the SM backgrounds

Concentrating on the squeezed spectrum with a small mass splitting with $\Delta m = 10\,\text{GeV}$, we require the following basic selection cuts to optimize the search

- The leading non b-jet with $p_T(j_1) > 120\,\text{GeV}$.
- A stringent cut on the transverse missing energy with $E_T^{\text{miss}} > E_{T,\text{min}}^{\text{miss}}$, where $E_{T,\text{min}}^{\text{miss}}$ varies to optimize the search.
- At least one b-jet with $p_T(b_1) > 25\,\text{GeV}$ and $|\eta| < 2.5$.
- No leptons including $\tau^{\pm}$ with $p_T > 20\,\text{GeV}$ and $|\eta| < 2.5$.

Here, the last cut is introduced to cut the dominant $t\bar{t}$ background, which turns to have one or more charged leptons in the final state. To further reduce the backgrounds, we have found three more useful variables.

The first variable is an upper limit cut on the leading b-jet. The reason for introducing this cut is because the leading b-jet p_T from the signal is less energetic than that from backgrounds. From the top quark backgrounds, the b-jet comes from the top quark decay. With a sufficiently large missing transverse cut like $E_T^{\text{miss}} > 400\,\text{GeV}$ in figure 3, the top quarks are slightly boosted and have the decay product b-jet to be energetic. For the $W, Z + \text{hf}$ backgrounds, the leading b-jet prefers to be energetic to be summed together with the leading non b-jet to match the large E_T^{miss}. For the signal, however, the missing transverse energy comes from two missing particles and both b-jet p_T's are needed to compensate the difference between E_T^{miss} and the leading non b-jet $p_T(j_1)$. As shown in the left panel of figure 3 for the distributions of fraction of events, the sbottom signal does have almost all events with $p_T(b_1)$ below 110 GeV, while for backgrounds some fractions of events have $p_T(b_1)$ above 110 GeV. We will later vary the upper limit cut on $p_T(b_1)$ to improve our signal reaches. To have also a rough idea about the sizes of different backgrounds, we also show the absolute signal and background cross section distributions in terms of $p_T(b_1)$ in the right panel of figure 3.

The second useful variable, $|\Delta\phi(p_T(b_1), E_T^{\text{miss}})|$, is the azimuthal angle difference between the leading b-jet p_T and E_T^{miss}. For the $V + bb$ background, the leading b-jet prefers to have the same moving direction as the leading non b-jet, which is opposite to the transverse missing energy direction, so the $|\Delta\phi(p_T(b_1), E_T^{\text{miss}})|$ distributions should peak at π for this background. For the $t\bar{t}$ and single top backgrounds, the leading b-jet can align or anti-align with E_T^{miss}, while for the sbottom signal the leading b-jet prefers to align with E_T^{miss}. The reason has already been illustrated at the beginning of section 2. In order to have a large missing energy, the ISR jet will boost both sbottoms and make the bottom quarks move in the same direction as their corresponding neutralinos. We show the signal and background $|\Delta\phi(p_T(b_1), E_T^{\text{miss}})|$ distributions in the left panel of figure 4 after imposing a cut on the missing transverse energy with $E_T^{\text{miss}} > 250\,\text{GeV}$, the actual value of this cut does not change the general features of signal and background distributions, as far as Δm is kept small.

JHEP08(2012)003

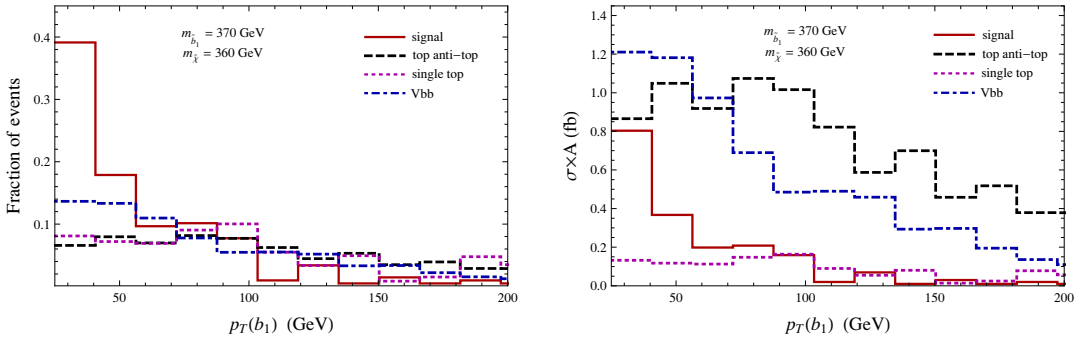

Figure 3. Left panel: the normalized fractions of events for the signal and backgrounds in terms of $p_T(b_1)$. Here, $m_{\tilde{b}_1} = 370\,\text{GeV}$ and $m_{\tilde{\chi}} = 360\,\text{GeV}$. The basic selection cuts with $E_T^{\text{miss}} > 400\,\text{GeV}$ have been imposed for all histograms. The signal acceptance is around 1.7%. Right panel: the same as the left one but for the absolute cross section distributions after the $E_T^{\text{miss}} > 400\,\text{GeV}$ cut.

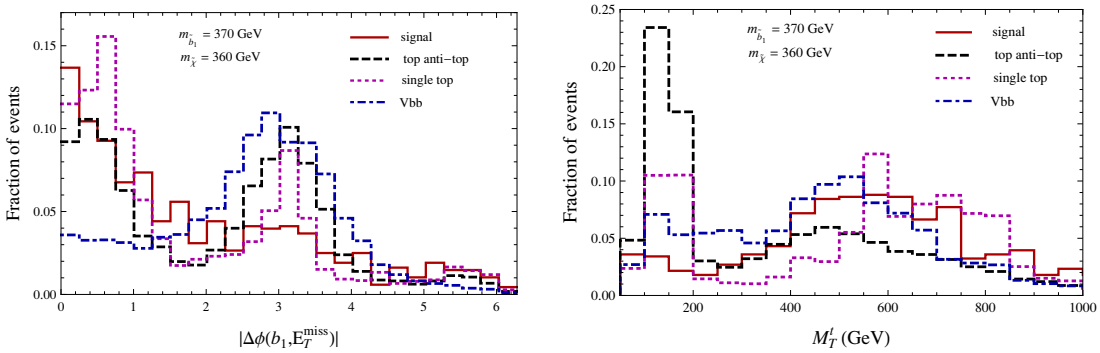

Figure 4. Left panel: the $|\Delta\phi(p_T(b_1), E_T^{\text{miss}})|$ distributions for the signal and backgrounds after imposing the basic selection cuts with $E_T^{\text{miss}} > 250\,\text{GeV}$. Right panel: the same as the left panel but for M_T^t distributions.

The third variable is called M_T^t or the top quark transverse mass. Since the $t\bar{t}$ background is one of the dominant backgrounds, reducing this background can definitely improve the final reach for sbottoms. It turns out that the dominant $t\bar{t}$ background is in the semi-leptonic channel with the lepton missing. So, this M_T^t is defined specifically for this part of backgrounds.[1] We define this variable as

$$M_T^t = \sqrt{\left[E_T(j_a) + \sqrt{(E_T^{\text{miss}})^2 + M_W^2}\right]^2 - \left|\mathbf{p_T}(j_a) + \mathbf{E_T^{\text{miss}}}\right|^2}\,, \tag{3.1}$$

where j_a is one of the three leading jets with $p_T > 25\,\text{GeV}$ including the leading b-jet (or the leading two b-jets). We choose j_a to be the one not belonging to the pair of jets with the smallest invariant mass among the three pairs. Since the lepton in the semi-leptonic $t\bar{t}$

[1] A similar but more complicated strategy for reducing the dileptonic $t\bar{t}$ background for the stop search, see ref. [26].

JHEP08(2012)003

background is missing to provide a large transverse missing energy with the neutrino, we use the W gauge boson mass for the missing particle. Noticing that there are two b-quarks in the final state at parton level for this background, one of the two b-quarks should come from the same top quark as the missing W. Because of the b-tagging efficiency from the detector simulations, there are more events with just one b-jet in the final state with the other b-jet either not tagged or too soft or too forward to pass the basic jet selection. Our way of selecting the right jet together with the missing W to calculate M_T^t is based on the fact that the two jets with the smallest invariant mass are more likely from the hadronic top and the remaining one is from the leptonic top. We show the M_T^t distributions of signal and background events in the right panel of figure 4. As one can see from the right panel of figure 4, the majority of the $t\bar{t}$ background indeed has M_T^t bounded by around the top quark mass, while the signal does have a good fraction of events with M_T^t much above the top quark mass. So, a big fraction of the $t\bar{t}$ background will be reduced later by imposing a lower limit cut on M_T^t.

At last, it should be noticed that the variables presented in this section, as well as the basic selection cuts previously defined, have correlations among them. Therefore, the results in figures 3, 4 are intended to pictorially illustrate the discriminating power of each variable separately after the selection cuts. The combined discriminating power of the variables and selection cuts will be analyzed in next section.

4 Discovery reach

In this section we use the general search strategy with one b-jet, one hard ISR jet and a large $E_T^{\rm miss}$ plus the three variables in the previous section to study the sbottom discovery or exclusion reach. All our results reported here are for the 8 TeV LHC with an expected $20\,{\rm fb}^{-1}$ luminosity.

We take two reference points in the $m_{\tilde{b}_1}$ and $m_{\tilde{\chi}}$ plane to study the optimization of the cuts. To fully apply the search strategy developed in previous section for the squeezed spectrum, we take the reference point 1 to have $m_{\tilde{b}_1} = 370\,{\rm GeV}$ and $m_{\tilde{\chi}} = 360\,{\rm GeV}$. Since the optimized cuts for this reference point with $\Delta m = 10\,{\rm GeV}$ are not efficient to cover the parameter space with a larger Δm, we also consider a second reference point with $m_{\tilde{b}} = 430\,{\rm GeV}$ and $m_{\tilde{\chi}} = 310\,{\rm GeV}$ in order to cover the medium Δm region between the squeezed spectrum and the large Δm region. We have verified that this point is outside of the reach of an extended analysis to $20\,{\rm fb}^{-1}$ using a search strategy similar as the one in ref. [10].

To choose the best set of cuts for each of the reference points, we scan the parameter space for different cuts in $E_T^{\rm miss}$, $|\Delta\phi(b_1, E_T^{\rm miss})|$, M_T^t and $p_T(b_1)$, and compute the numbers of signal (S) and background (B) events expected in $20\,{\rm fb}^{-1}$ of luminosity at the 8 TeV LHC. The details of the simulation have been depicted in section 2. The Poisson probability that B events purely from backgrounds would fluctuate up to at least $S+B$ events is given by ROOT's two-parameter Γ function, which can be evaluated at non-integer parameters:

$$p \;=\; \sum_{k=S+B}^{\infty} \frac{B^k}{k!} e^{-B} \;=\; \texttt{TMath}::\texttt{Gamma}(S+B, B)\;. \tag{4.1}$$

JHEP08(2012)003

$E_T^{\rm miss} >$ (GeV)	$M_T^t >$ (GeV)	$\lvert\Delta\phi(b_1, E_T^{\rm miss})\rvert <$	$p_T(b_1) <$ (GeV)	$\sigma_{t\bar{t}}$ (fb)	σ_{tX} (fb)	$\sigma_{Vb\bar{b}}$ (fb)	σ_B (fb)	σ_S (fb)	significance ($20\,\text{fb}^{-1}, 8\,\text{TeV}$)
430	—	—	—	8.2	0.3	5.9	14.4	1.5	1.7
430	200	—	—	5.0	0.3	5.5	10.8	1.4	1.9
430	200	1.8	—	2.3	0.2	1.1	3.6	1.0	2.4
430	200	1.8	100	1.1	0.1	0.7	1.9	1.0	2.9

Table 1. Optimized cuts for the reference point 1 with $m_{\tilde{b}_1} = 370\,\text{GeV}$ and $m_{\tilde{\chi}} = 360\,\text{GeV}$. The branching ratio of $\tilde{b}_1 \to b\tilde{\chi}$ is chosen to be 100%. The last column represents the significance for each set of cuts expected at $20\,\text{fb}^{-1}$ of the 8 TeV LHC.

We translate this probability into a gaussian-equivalent significance (σ) in terms of standard deviations. This approaches $S/\sqrt{B}$ for a large signal and background. We select the best set of cuts for each reference point as the one that would maximize the significance and then apply the same cuts to other masses as well.

To understand better the effects of different cuts on the signal and backgrounds, we present in table 1 how the significance increases as the different cuts are imposed in succession for the reference point 1. The basic cuts on other objects in the final state have been imposed and described at the beginning of section 3. Besides vetoing any event containing at least one charged lepton (including tau's), we begin with an overall stringent cut of $E_T^{\rm miss} > 430\,\text{GeV}$ to boost the sbottom system. In agreement with the analyses in the previous section, a cut inspired in the right panel of figure 4 of $M_T^t > 200\,\text{GeV}$ reduces the main $t\bar{t}$ background by about one half. We then see that a cut in the angular variable with $|\Delta\phi(b_1, E_T^{miss})| < 1.8$ discards most of the Vbb background and reduces one half of the $t\bar{t}$ and single-top backgrounds tX, as expected from the left panel in figure 4. A final upper-limit cut in the transverse momentum of the leading b-jet of $p_T(b_1) < 100\,\text{GeV}$ further reduces the total background by around one half while not affecting the signal, in concordance with the analysis in figure 3. The combination of all these cuts enhances the significance for this reference point from 1.7 to 2.9 standard deviations. In our current study, we have neglected potential systematic errors from a realistic experimental search. Moreover, since this analysis relies on ISR, there will also be a new source of systematic errors coming from the Monte Carlo modeling of ISR. However, since the three variables used in table 1 can increase S/B from 0.1 to 0.5, we anticipate that our variables are also useful to decrease the systematic errors.

For the reference point 2, where the mass gap is $\Delta m = 120\,\text{GeV}$, the upper cut on $p_T(b_1)$ is not so useful because the signal events turn to have large values of $p_T(b_1)$. Similarly, a large missing transverse energy can be obtained without boosting sbottoms too much. The angular cut on $|\Delta\phi(b_1, E_T^{\rm miss})|$ is not a characterization of the signal any more, since for this case the b does not need to be aligned with $\tilde{\chi}$ in the lab system. Therefore, we don't use those two new variables: an upper cut on $p_T(b_1)$ and a lower cut on $|\Delta\phi(b_1, E_T^{\rm miss})|$. Although the background events still have a peak structure for $2.5 \leq |\Delta\phi(b_1, E_T^{\rm miss})| \leq 3.5$ as the distribution in the left panel of figure 4, we have

JHEP08(2012)003

$E_T^{miss} >$ (GeV)	$M_T^t >$ (GeV)	$\sigma_{t\bar{t}}$ (fb)	σ_{tX} (fb)	$\sigma_{Vb\bar{b}}$ (fb)	σ_B (fb)	σ_S (fb)	significance ($20\,\text{fb}^{-1}, 8\,\text{TeV}$)
270	-	87.1	5.7	52.2	145.0	5.9	2.2
270	200	50.1	5.0	47.5	102.6	5.4	2.4

Table 2. The same as table 1, but for the reference point 2 with $m_{\tilde{b}_1} = 430\,\text{GeV}$ and $m_{\tilde{\chi}} = 310\,\text{GeV}$. Due to a larger mass gap compared to the reference point 1 in table 1, cuts of $|\Delta\phi(b_1, E_T^{\text{miss}})|$ and $p_T(b_1)$ are found to be not useful for this point.

found that imposing a cut with $2.5 \leq |\Delta\phi(b_1, E_T^{\text{miss}})| \leq 3.5$ can not increase the discovery sensitivity. For the transverse momentum of the leading b-jet, we have found that it does not have a clear upper bound that can differentiate the signal from backgrounds. For this middle size of mass gaps, we have found that the only cuts that increase the significance are vetoing any charged leptons, a sufficiently large missing transverse momentum cut, and a lower cut on M_T^t to reduce the top background. We show in table 2 the optimal cuts for the reference point 2 as well as the effects of the M_T^t cut on reducing the $t\bar{t}$ backgrounds and increasing the final significance.

After finding the optimized cuts for these two reference points in tables 1 and 2, we apply them to other model parameter space of the $m_{\tilde{b}_1}$ and $m_{\tilde{\chi}}$ plane. We show the discovery significance in the left and right panels of figure 5 using the two reference cuts, respectively. In figure 5, the dashed line along the diagonal line is the kinematically forbidden limit, above which $\tilde{b}_1$ can no longer have a two-body decay into $\tilde{\chi}$ plus a b quark at the parton level. Since the existing Monte Carlo programs do not cover this highly squeezed region precisely, we only simulate the parameter region with $\Delta m \geq 10\,\text{GeV}$ in our studies. The simulation boundary is shown as the solid line in the diagonal direction in figure 5. We leave the discussion of the extremely squeezed region with $5 \lesssim \Delta m < 10\,\text{GeV}$ in the next section.

From the left panel of figure 5, we see that the optimized search strategy for the reference point 1 with $\Delta m = 10\,\text{GeV}$ produces an abrupt enhancement in a region which is parallel and close to the $\Delta m = 10\,\text{GeV}$ line. This can be understood from the set of cuts designed for this point: the upper bound on $p_T(b_1)$ and the cut on $|\Delta\phi(b_1, E_T^{\text{miss}})|$ differentiate signal from background only when Δm is sufficiently small. On the other hand, if Δm is too small, a larger boost from the ISR jet is required to increase the missing transverse energy to reduce the backgrounds. The signal production cross section decreases as the ISR jet increases, so the significance also becomes worse. The actual reduction on significance depends on the sbottom masses. For a heavier $\tilde{b}_1$, a larger reduction of significance on the diagonal boundary of the left panel of figure 5 is anticipated. As one can see from this panel, the highly squeezed region has a better coverage than the region with a large splitting. At 95% C.L., one can exclude $m_{\tilde{b}_1}$ up to 400 GeV even when the mass splitting is as small as $\Delta m \approx 10\,\text{GeV}$.

The right panel in figure 5, on the other hand, has a slightly different pattern due to different reference cuts. In this plot, for a fixed $m_{\tilde{b}_1}$ the significance decreases monotonically

JHEP08(2012)003

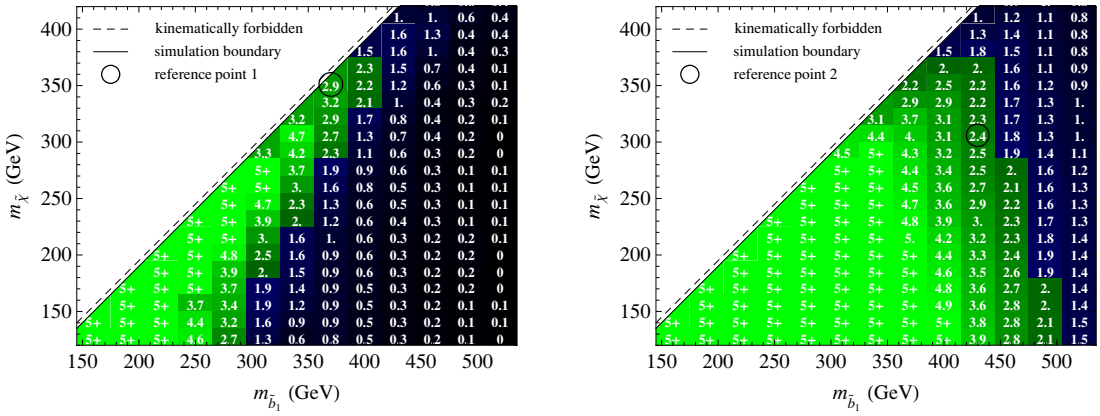

Figure 5. Significance expected for 20 fb^{-1} luminosity at the 8 TeV LHC for different sets of $m_{\tilde{b}_1}$ and $m_{\tilde{\chi}}$ using the optimal cuts found for the reference point 1 (left panel) and the reference point 2 (right panel). See tables 1 and 2 for detailed cuts.

as $m_{\tilde{\chi}}$ increases. Because no cuts on $p_T(b_1)$ and $|\Delta\phi(b_1, E_T^{\rm miss})|$ have been applied for the reference point 2, we don't anticipate a similar pattern as the left panel. From the right panel, we can see that even though the set of cuts for the reference point 2 is not optimized for the highly squeezed region, a wide range of parameter space with a small Δm can still be covered. Furthermore, this set of cuts can also cover the parameter region with a large Δm. Our results show that for a large Δm above 300 GeV one can exclude $\tilde{b}_1$ up to 500 GeV at 95% C.L. We also want to emphasize that the set of cuts for the reference 2 is not optimized for the large Δm region. The search strategy used in the ATLAS existing search [10] by requiring two hard b-jets is the right one to cover this region.

Since both panels in figure 5 have used the general search strategy by requiring 1 or 2 not-so-hard b-jets with one energetic ISR jet and a large $E_T^{\rm miss}$, it is not surprise that both can cover the highly squeezed spectra. Comparing the two results from the left panel and the right panel, we can see that the cuts used for the reference point 2 can cover most the squeezed spectra, while the cuts for the reference point 1 can have a better limit for the extreme cases with $\Delta m \approx 10$ GeV. Moreover, one can see from table 2 that the optimization for the reference point 2 comes mainly from the selection cuts. One may expect a good performance in this region without the kinematic variables defined in section 3. These variables, instead, are useful to optimize the performance in the squeezed spectrum.

In order to compare our results to a search strategy like the one used in ref. [10], we have also calculated the projected 95% C.L. exclusion limit by cutting the first and second leading b-jet p_T's to be above 170 and 80 GeV respectively, and requiring $E_T^{\rm miss} \geq 200$ GeV with all other cuts including the cut on m_{CT} left the same. The result is shown in the red dot-dashed line in figure 6. To combine the reach limits from using the two reference cuts in figure 5 we take the larger significance for a given $m_{\tilde{b}_1}$ and $m_{\tilde{\chi}}$. The 95% C.L. exclusion limit is shown in the red solid line in figure 6. Comparing the regions covered by our search strategy and the projection of the existing search strategy at the 8 TeV LHC with

JHEP08(2012)003

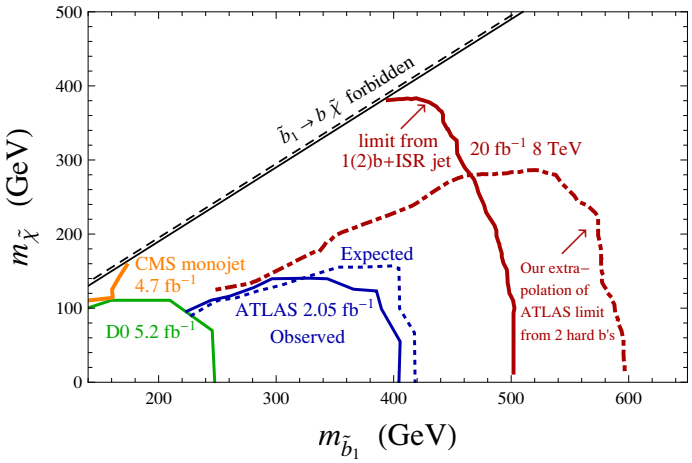

Figure 6. The projected 95% C.L. exclusion limits from our search strategy are shown in the red solid line for the 8 TeV LHC at 20 fb^{-1}. Our extrapolation of the existing search strategy by requiring two hard b-jets is shown in the red dot-dashed line with the same luminosity. All other limits from existing experimental searches are also at 95% C.L.

20 fb^{-1}, the dotdashed red line in figure 6, we have found that a wide squeezed spectrum region, which is not covered by the projection of the existing strategy, is now covered by our proposal. Interestingly, the existing and our new search strategies are complimentary to each other in a sense that the existing search strategy has a better coverage for the large Δm region.

In figure 6, we also show existing experimental limits on the $m_{\tilde{b}_1}$ and $m_{\tilde{\chi}}$ plane. The blue solid and blue dotted lines are 95% C.L. observed and expected exclusion limits from the ATLAS search results with 2.05 fb^{-1} luminosity at the 7 TeV LHC [10]. The green solid line is from the D0 search with 5.2 fb^{-1} at the 1.96 TeV Tevatron [9]. In the orange solid line, we show the 95% C.L. limit from the mono-jet search results from CMS with 4.7 fb^{-1} luminosity at the 7 TeV LHC and using their $E_T^{\rm miss} > 350$ GeV cut [15]. The simple mono-jet search is not optimized to cover the squeezed sbottom-neutralino spectra. We note that there are also other supersymmetry searches [27–30] including using the Razor variable [31] that could cover some part of the parameter space in figure 6 when projected to the 2012 run and/or when adapted to the specific sbottom search.

5 Discussion and conclusions

All our studies in this paper have the sbottom-neutralino mass splitting Δm above 10 GeV. For the case of a smaller mass-splitting, the physics is more complicated but also interesting. When the mass splitting is reduced to be close but above the lightest B-hadron mass around 5.3 GeV, we anticipate that sbottom should decay into neutralino plus a single B-hadron. With the boost of the ISR jet, the signature of this region of parameter space should be one ISR jet, a large missing transverse momentum plus two single B-hadrons. The single B-hadron jet is different from the ordinary b-jet from QCD and can be tagged using a method

JHEP08(2012)003

beyond the standard b-jet tagging algorithm by requiring less tracks for the b-tagged jet. For the mass splitting below the mass of the lightest B-hadron, sbottom should have a multi-body decay into lighter hadrons plus neutralino.

For the parameter region with a large $m_{\tilde{b}_1}$ and also a large Δm, one may think about studying the single sbottom production in association with a neutralino as $g\,b \to \tilde{b}_1\,\tilde{\chi}$. One may gain some production cross section by only producing one heavy particle in the final state. The final state is a mono-b jet plus missing transverse energy. However, comparing to the pair-production of $\tilde{b}_1$, two additional reduction factors make the single sbottom production cross section very small. One is the small coupling among b-quark, $\tilde{b}_1$ and $\tilde{\chi}$ in comparison with the QCD coupling. The other one is the smallness of the fraction of the b-parton inside the proton. We have checked that the ratio of the single sbottom production cross section over the pair-production one is around 10^{-3} to 10^{-2} for $m_{\tilde{b}_1}$ from 600 GeV to 1 TeV, with a fixed the neutralino mass as 100 GeV.

In summary, we have proposed a new search strategy to cover the squeezed spectrum with a small mass difference between sbottom and neutralino. The general search strategy of our proposal requires one hard ISR jet, one or two b-jets with a medium value of p_T's and a large transverse missing energy. To further improve the search limit in the squeezed spectrum, we have found several useful variables including the azimuthal angle difference between the leading b-jet and $E_T^{\rm miss}$ and the top quark transverse mass M_T^t, defined in terms of a b-jet and the missing W for the $t\bar{t}$ background. With a $20\,{\rm fb}^{-1}$ luminosity at the 8 TeV LHC we have found that, neglecting systematic errors, our new search strategy can cover a wide range of parameter space with $\Delta m \lesssim 200\,{\rm GeV}$ that would have not been covered by extending previous analysis. Although our studies show that systematic errors could be reduced, we may expect new sources of systematic errors from the ISR modeling which are not present in the previous analysis. Moreover, a verification of the ISR modeling by the LHC experiments, which has not been done because the experimentalists are cautious about understanding of the ISR, could be required for a full application of the search strategy proposed here. For a very small mass splitting with $\Delta m \approx 10\,{\rm GeV}$, we have found that the sbottom with a mass up to 400 GeV can be excluded at 95% C.L.. Using the previous analysis strategy by requiring two hard b-jets, we estimate the reach for the sbottom mass to be around 600 GeV for $\Delta m \gtrsim 300\,{\rm GeV}$.

Acknowledgments

We would like to thank Bart Clayton Butler, Michael Peskin, Ariel Schwartzman, Daniel Silverstein and Peter Skands for useful discussion and comments. SLAC is operated by Stanford University for the US Department of Energy under contract DE-AC02-76SF00515. The author EA thanks Conicet for the special funding.

JHEP08(2012)003

References

[1] ATLAS collaboration, *Observation of an excess of events in the search for the standard model Higgs boson with the ATLAS detector at the LHC*, ATLAS-CONF-2012-093 (2012).

[2] CMS collaboration, *Evidence for a new state decaying into two photons in the search for the standard model Higgs boson in pp collisions*, PAS-HIG-12-015 (2012).

[3] CMS collaboration, *Evidence for a new state in the search for the standard model Higgs boson in the $H \to ZZ \to 4$ leptons channel in pp collisions at $\sqrt{s} = 7$ and 8 TeV*, PAS-HIG-12-016 (2012).

[4] S. Dimopoulos and G. Giudice, *Naturalness constraints in supersymmetric theories with nonuniversal soft terms*, *Phys. Lett.* **B 357** (1995) 573 [hep-ph/9507282] [INSPIRE].

[5] A.G. Cohen, D. Kaplan and A. Nelson, *The more minimal supersymmetric standard model*, *Phys. Lett.* **B 388** (1996) 588 [hep-ph/9607394] [INSPIRE].

[6] P. Lodone, *Supersymmetry phenomenology beyond the MSSM after $5\,fb^{-1}$ of LHC data*, *Int. J. Mod. Phys.* **A 27** (2012) 1230010 [arXiv:1203.6227] [INSPIRE].

[7] H.M. Lee, V. Sanz and M. Trott, *Hitting sbottom in natural SUSY*, *JHEP* **05** (2012) 139 [arXiv:1204.0802] [INSPIRE].

[8] CDF collaboration, T. Aaltonen et al., *Search for the production of scalar bottom quarks in $p\bar{p}$ collisions at $\sqrt{s} = 1.96$ TeV*, *Phys. Rev. Lett.* **105** (2010) 081802 [arXiv:1005.3600] [INSPIRE].

[9] D0 collaboration, V.M. Abazov et al., *Search for scalar bottom quarks and third-generation leptoquarks in $p\bar{p}$ collisions at $\sqrt{s} = 1.96$ TeV*, *Phys. Lett.* **B 693** (2010) 95 [arXiv:1005.2222] [INSPIRE].

[10] ATLAS collaboration, G. Aad et al., *Search for scalar bottom pair production with the ATLAS detector in pp collisions at $\sqrt{s} = 7$ TeV*, *Phys. Rev. Lett.* **108** (2012) 181802 [arXiv:1112.3832] [INSPIRE].

[11] J. Alwall, J.L. Feng, J. Kumar and S. Su, *B's with direct decays: Tevatron and LHC discovery prospects in the $b\bar{b}$ + MET channel*, *Phys. Rev.* **D 84** (2011) 074010 [arXiv:1107.2919] [INSPIRE].

[12] M. Adeel Ajaib, T. Li and Q. Shafi, *Searching for NLSP sbottom at the LHC*, *Phys. Lett.* **B 701** (2011) 255 [arXiv:1104.0251] [INSPIRE].

[13] M.R. Buckley, L. Randall and B. Shuve, *LHC searches for non-chiral weakly charged multiplets*, *JHEP* **05** (2011) 097 [arXiv:0909.4549] [INSPIRE].

[14] CDF collaboration, T. Aaltonen et al., *A Search for dark matter in events with one jet and missing transverse energy in $p\bar{p}$ collisions at $\sqrt{s} = 1.96$ TeV*, *Phys. Rev. Lett.* **108** (2012) 211804 [arXiv:1203.0742] [INSPIRE].

[15] CMS collaboration, *Search for dark matter and large extra dimensions in monojet events in pp collisions at $\sqrt{s} = 7$ TeV*, EXO-11-059 (2011).

[16] J. Alwall, M. Herquet, F. Maltoni, O. Mattelaer and T. Stelzer, *MadGraph 5: going beyond*, *JHEP* **06** (2011) 128 [arXiv:1106.0522] [INSPIRE].

[17] T. Sjöstrand, S. Mrenna and P.Z. Skands, *PYTHIA 6.4 physics and manual*, *JHEP* **05** (2006) 026 [hep-ph/0603175] [INSPIRE].

JHEP08(2012)003

[18] J.S. Conway, *Pretty good simulation of high-energy collisions*, 090401 release.

[19] M. Cacciari, G.P. Salam and G. Soyez, *The anti-k_t jet clustering algorithm*, *JHEP* **04** (2008) 063 [arXiv:0802.1189] [INSPIRE].

[20] J. Alwall et al., *Comparative study of various algorithms for the merging of parton showers and matrix elements in hadronic collisions*, *Eur. Phys. J.* **C 53** (2008) 473 [arXiv:0706.2569] [INSPIRE].

[21] W. Beenakker et al., *Squark and gluino hadroproduction*, *Int. J. Mod. Phys.* **A 26** (2011) 2637 [arXiv:1105.1110] [INSPIRE].

[22] N. Kidonakis, *Next-to-next-to-leading soft-gluon corrections for the top quark cross section and transverse momentum distribution*, *Phys. Rev.* **D 82** (2010) 114030 [arXiv:1009.4935] [INSPIRE].

[23] R. Schwienhorst, C.-P. Yuan, C. Mueller and Q.-H. Cao, *Single top quark production and decay in the t-channel at next-to-leading order at the LHC*, *Phys. Rev.* **D 83** (2011) 034019 [arXiv:1012.5132] [INSPIRE].

[24] R. Frederix et al., *W and $Z/\gamma*$ boson production in association with a bottom-antibottom pair*, *JHEP* **09** (2011) 061 [arXiv:1106.6019] [INSPIRE].

[25] F. Febres Cordero, L. Reina and D. Wackeroth, *W- and Z-boson production with a massive bottom-quark pair at the Large Hadron Collider*, *Phys. Rev.* **D 80** (2009) 034015 [arXiv:0906.1923] [INSPIRE].

[26] Y. Bai, H.-C. Cheng, J. Gallicchio and J. Gu, *Stop the top background of the stop search*, *JHEP* **07** (2012) 110 [arXiv:1203.4813] [INSPIRE].

[27] CMS collaboration, *Search for supersymmetry in all-hadronic events with missing energy*, CMS-PAS-SUS-11-004 (2011).

[28] CMS collaboration, *Search for supersymmetry in hadronic final states using MT2 with the CMS detector at 7 TeV*, CMS-PAS-SUS-12-002 (2012).

[29] CMS collaboration, *Search for supersymmetry with the razor variables at CMS*, CMS-PAS-SUS-12-005 (2012).

[30] CMS collaboration, S. Chatrchyan et al., *Search for supersymmetry at the LHC in events with jets and missing transverse energy*, *Phys. Rev. Lett.* **107** (2011) 221804 [arXiv:1109.2352] [INSPIRE].

[31] C. Rogan, *Kinematical variables towards new dynamics at the LHC*, arXiv:1006.2727 [INSPIRE].

JHEP08(2012)003